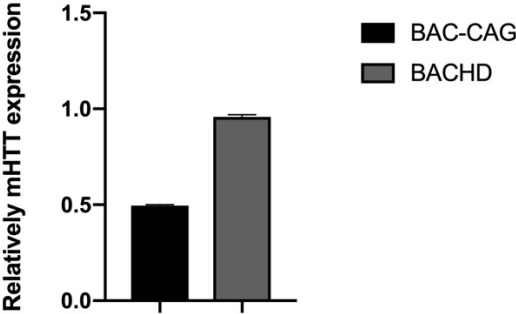


Gu et al. Supplemental Figures

Supplemental Figure S1

A



B

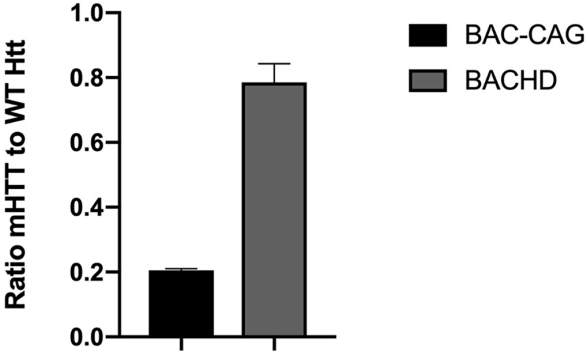
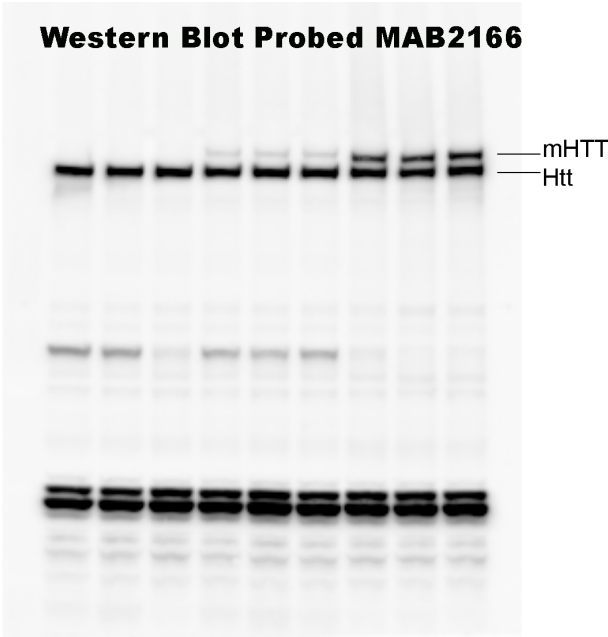
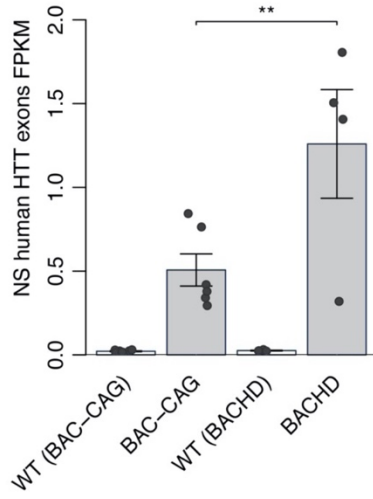


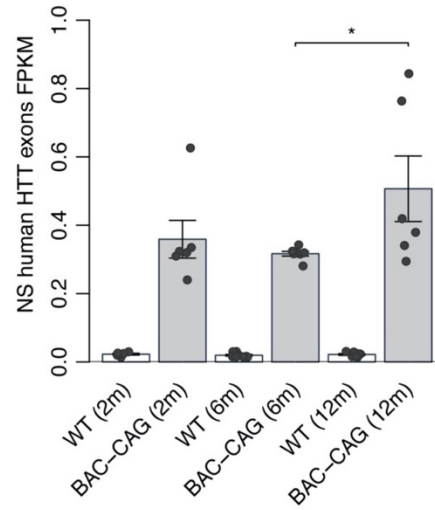
Figure S1 (Related to Figure 1). Quantitation of mHTT expression in BAC-CAG mice. (A) Quantification of mHTT bands in BAC-CAG and BACHD probed with 1C2 antibody. BAC-CAG expressed about half of mHTT proteins compared with BACHD. (B) The same membrane used for 1C2 antibody was striped and re-probed with MAB2166 antibody which able to detects both mutant human huntingtin and mouse endogenous huntingtin proteins on epitope outside of polyQ region. Quantification of mHTT bands indicated BAC-CAG expressed about 20% of mHTT proteins compared to BACHD. Results are shown as mean \pm SEM

Supplemental Figure S2

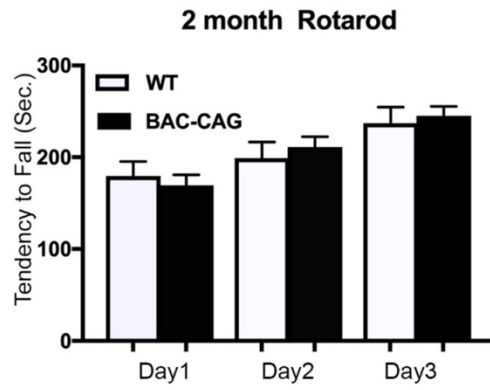
A



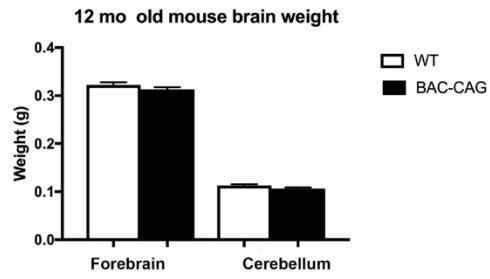
B



C



D



E

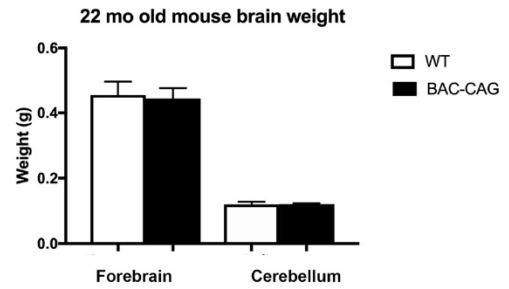
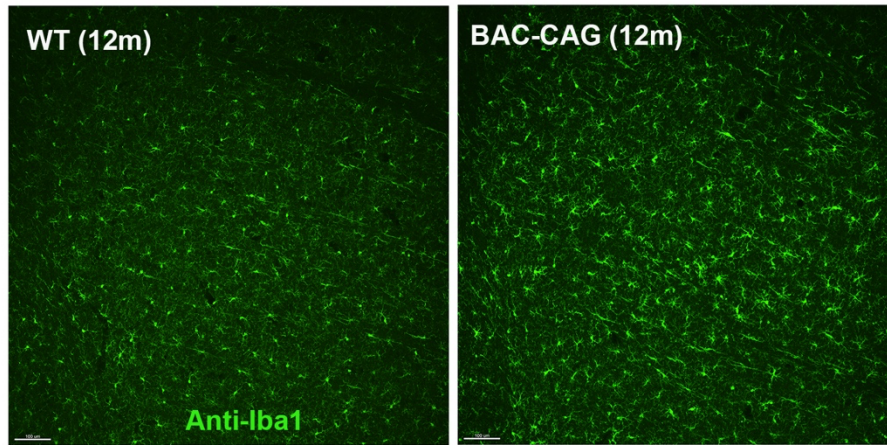


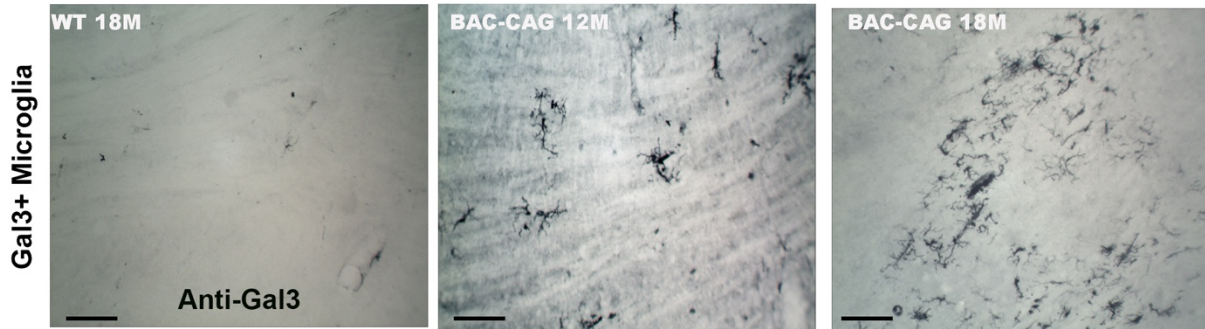
Figure S2 (Related to Figure 1). Characterization of BAC-CAG human HTT transcript reads, rotarod performance at 2m of age, and brain weights. (A, B). Reads corresponding to *HTT* exons and introns from RNA-seq datasets were added for BAC-CAG and BACHD and their WT controls, respectively. (A) BACHD showed significantly higher human *HTT* reads compared to BAC-CAG in the striatum at 12m of age. (B) BAC-CAG showed a modest but significant increase in human *HTT* transcript reads at 12m compared to 6m. Wildtype controls do not show any human *HTT* reads. Bars show means, error bars: std. error of the mean and dots the individual observations ($n = 6$ per genotype except $n = 4$ for BACHD genotype). ANOVA followed by Tukey HSD test was used to test differences among the transgenic samples only. * $p < 0.05$, **: $p < 0.01$). (C). Normal rotarod performance in 2m BAC-CAG mice compared to their WT littermates. Two-way ANOVA, no interaction between genotypes and times [$F(30, 36)=0.3188$, $p=0.9990$; BAC-CAG=16, WT=12]. Results are shown as mean \pm SEM. (D, E). Forebrain and cerebellum were weighted and no significant difference were detected at both 12 month (A) and 22 month (B) old of ages (12 month: BAC-CAG $n=12$, WT $n=14$; 22 month: BAC-CAG $n=8$, WT $n=7$). Results are shown as mean \pm SEM.

Supplemental Figure S3

A



B



C

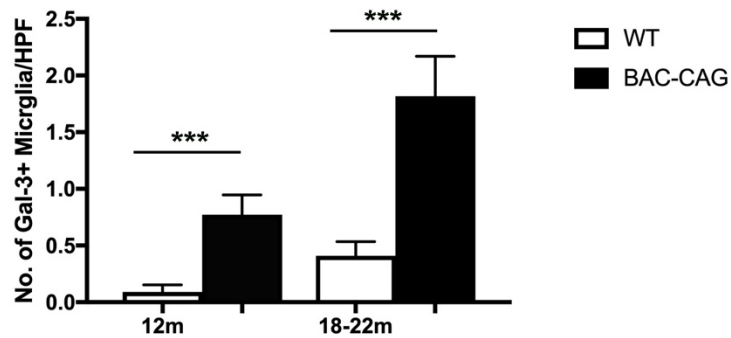
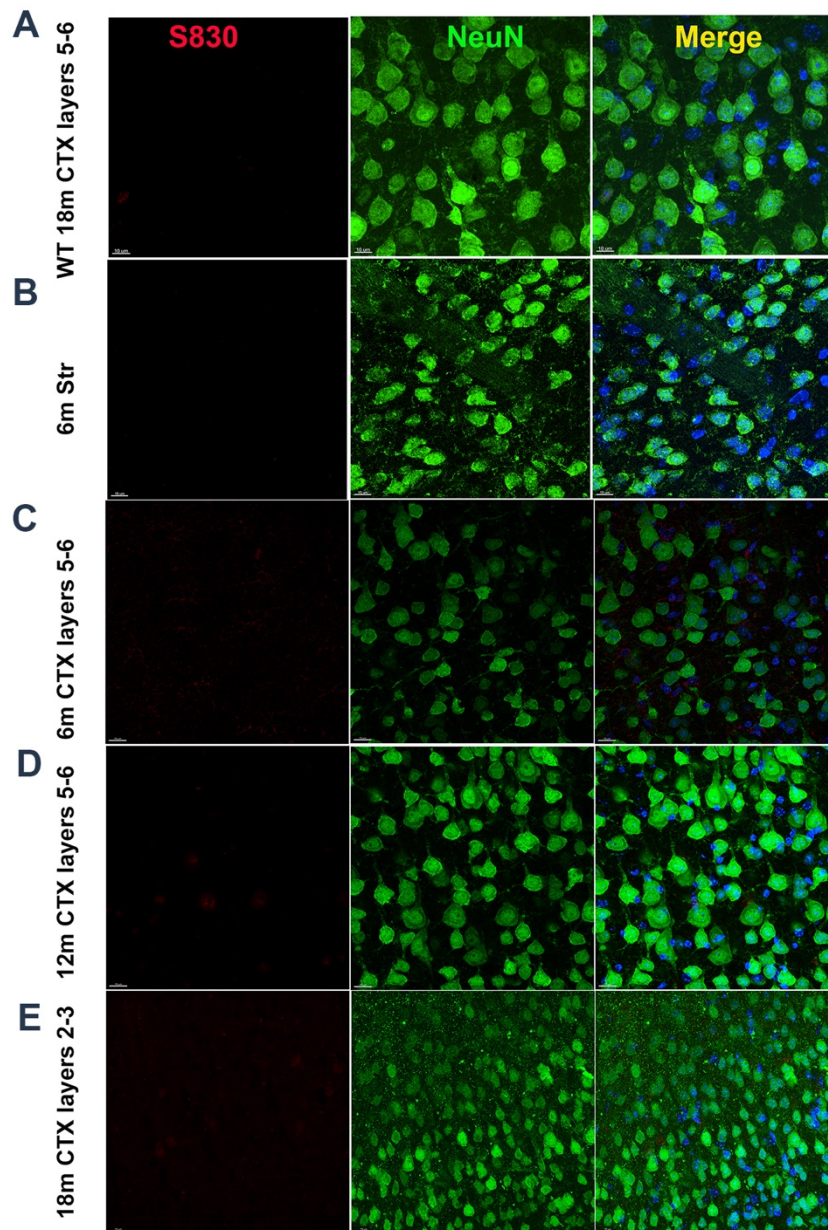


Figure S3 (Related to Figure 2). Microgliosis in BAC-CAG mice. (A) BAC-CAG mice displayed more and flamed-like Iba1(+) microglia, especially at globus pallidus. (B and C) BAC-CAG mice exhibited higher number of reactive microglia marker galactin 3(+) cells than those cells in WT controls. Results are shown as mean \pm SEM. Unpaired *t* test. *** $p < 0.005$. Scale Bar. 100 μ m

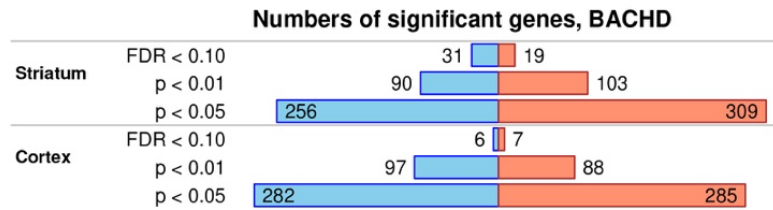
Supplemental Figure S4



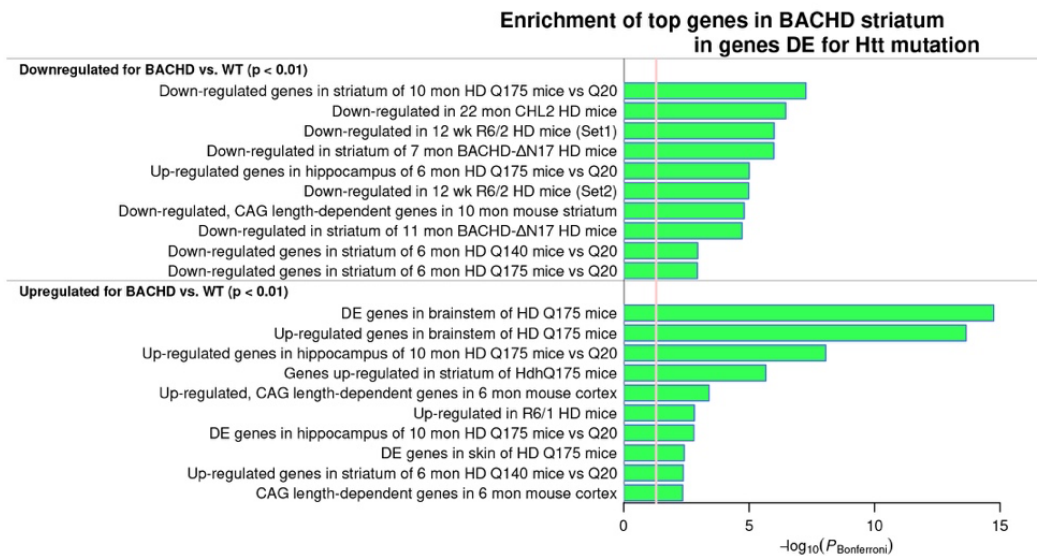
Supplemental Figure S4 (Related to Figure 3). Absence of Mutant HTT aggregation in WT and in the cortices of BAC-CAG mice (Related to Figure 3). No detections of S830(+) mHTT aggregates or nuclear inclusions in 18m WT brains (A). They were also absent in 6m old BAC-CAG mice (B,C). There were lack of positive signals in the deeper cortical layers (layers 5-6) (D) of 12m old, nor in the upper cortical layers (layers 2-3) of the 18m old (E) BAC-CAG mouse brains.

Supplemental Figure S5

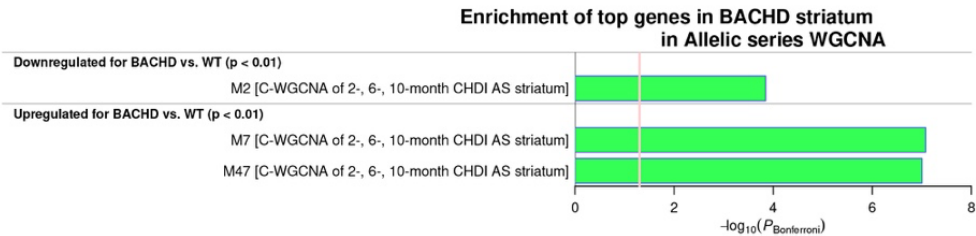
A



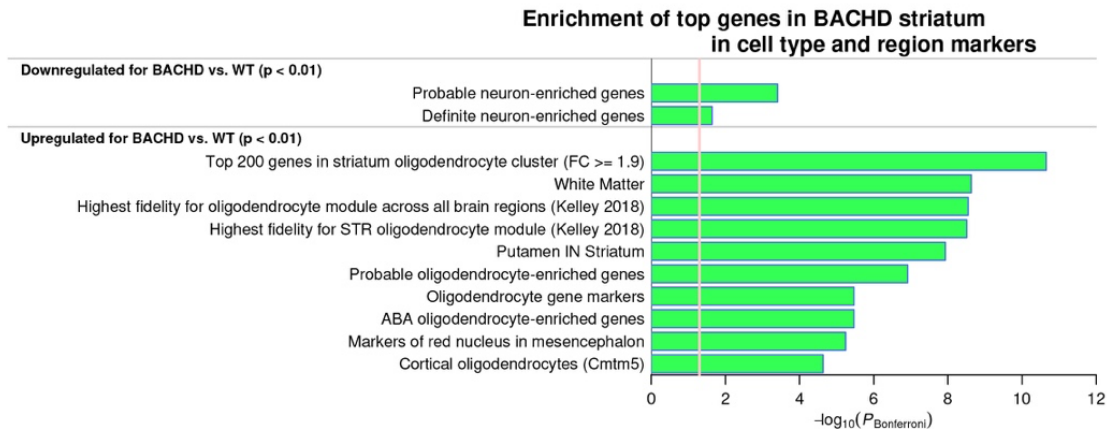
B



C

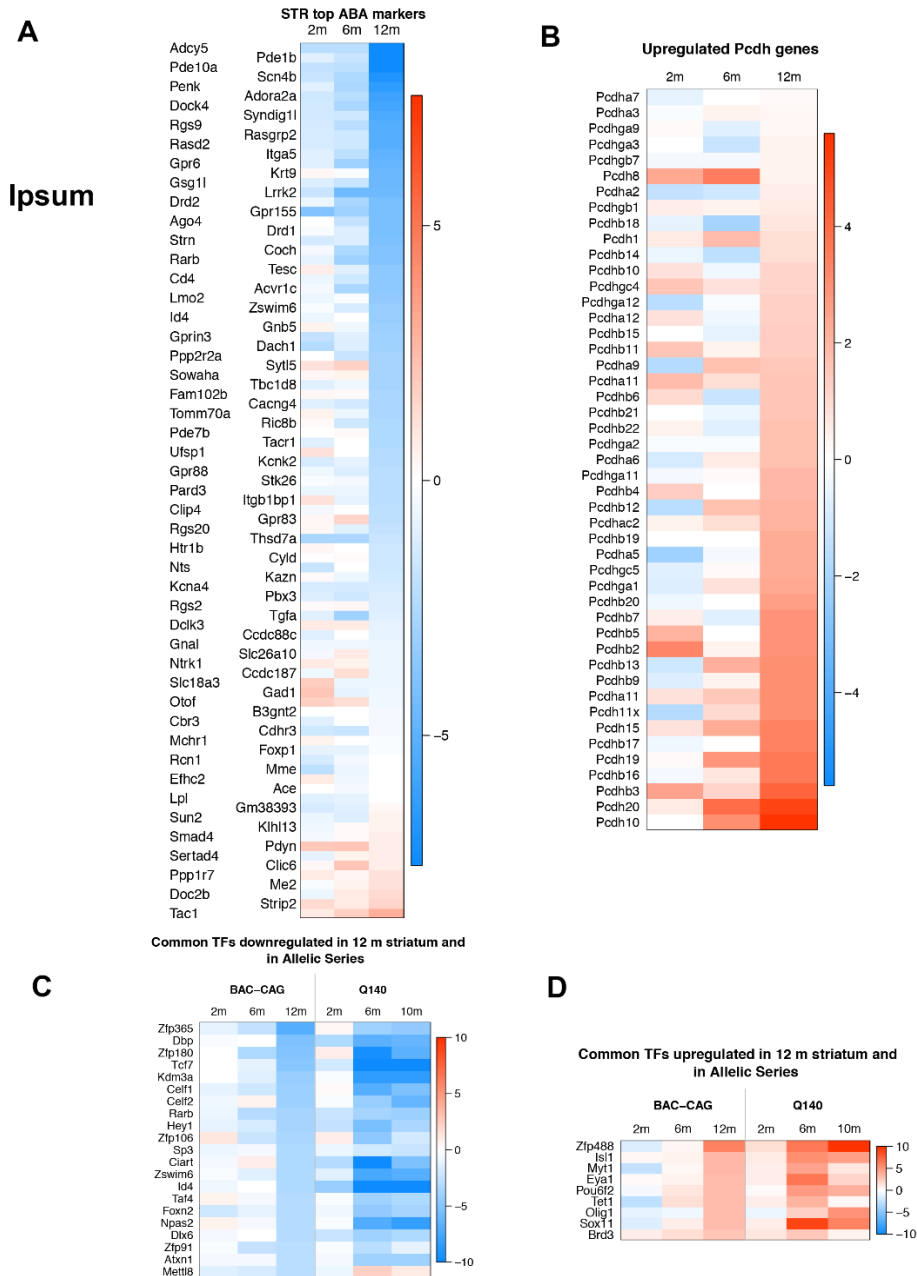


D



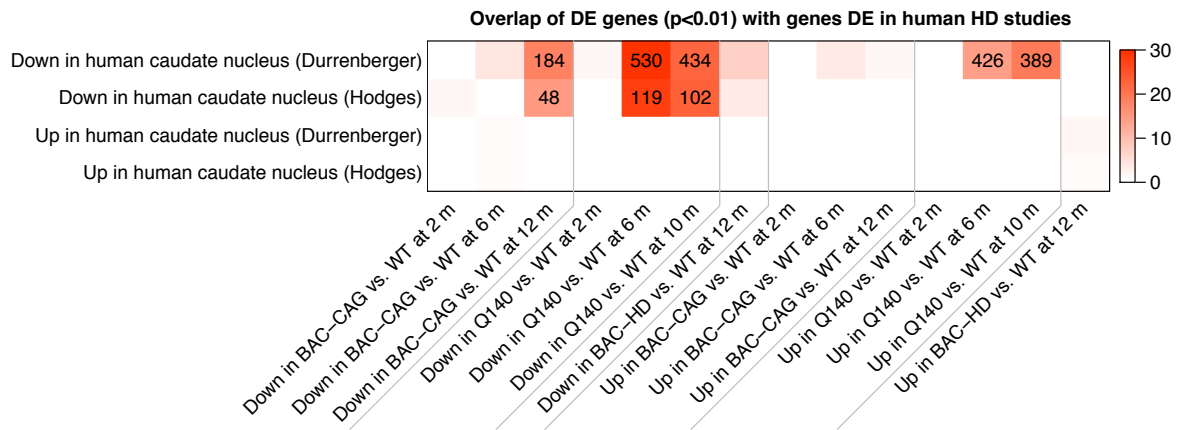
Supplemental Figure S5. (Related to Figure 4). Transcriptomic analysis of BACHD mice at 12-month of age. BAC-CAG mice RNA-seq analysis of cortex and striatum of BACHD and WT littermate controls at 12 months of age (N=4 per genotype, sex balanced). (A). The number of downregulated (Blue) and upregulated DE genes at different statistical thresholds between BACHD and WT controls. (B-D). Enrichment analysis of genes DE between BACHD and WT at $P < 0.01$ in 12-month striatum. Calculations were carried out using the anRichment R package. The top significantly enriched terms from transcriptomic signatures of HD mice (B), WGCNA modules from analysis of Htt CAG repeat knock-in Allelic Series (Langfelder et al., 2016) (C), and cell type and brain region markers (D) are shown.

Supplemental Figure S6



Supplemental Figure S6 (Related to Figure 4). Striatal transcriptomic dysregulation in BAC-CAG mice at 12m compared to wildtype littermate controls All heatmaps show DE Z statistics (log fold changes divided by their standard errors). (A). The pan-neuronal marker genes based on Allen Brain Atlas (ABA) are not consistently downregulated in BAC-CAG striata at 12m, a finding that is similar to the allelic series KI mice (Langfelder et al., 2016). (B). Upregulated clustered protocadherin genes are mainly significantly upregulated at 12m but not at 2m and 6m in BAC-CAG striata, a finding that is reminiscent of that in the allelic series KI mice (Langfelder et al., 2016). (C), (D) Transcription factors, chromatin factors and RNA binding proteins downregulated (C) and upregulated (D) in both BAC-CAG and Q140 KI mice.

Supplemental Figure S7



Supplemental Figure S7 (Related to Figure 4). Overlaps of genes DE at $p < 0.01$ in BAC-CAG and BACHD models with genes DE in studies of HD patients. The heatmap color indicates $-\log_{10}$ of the enrichment p-value (hypergeometric test) and numbers give overlap sizes for pairs with $p < 10^{-8}$. The human studies are (Hodges et al., 2006) and (Durrenberger et al., 2014) and both used the $FDR < 0.05$ threshold.

Supplemental Figure S8

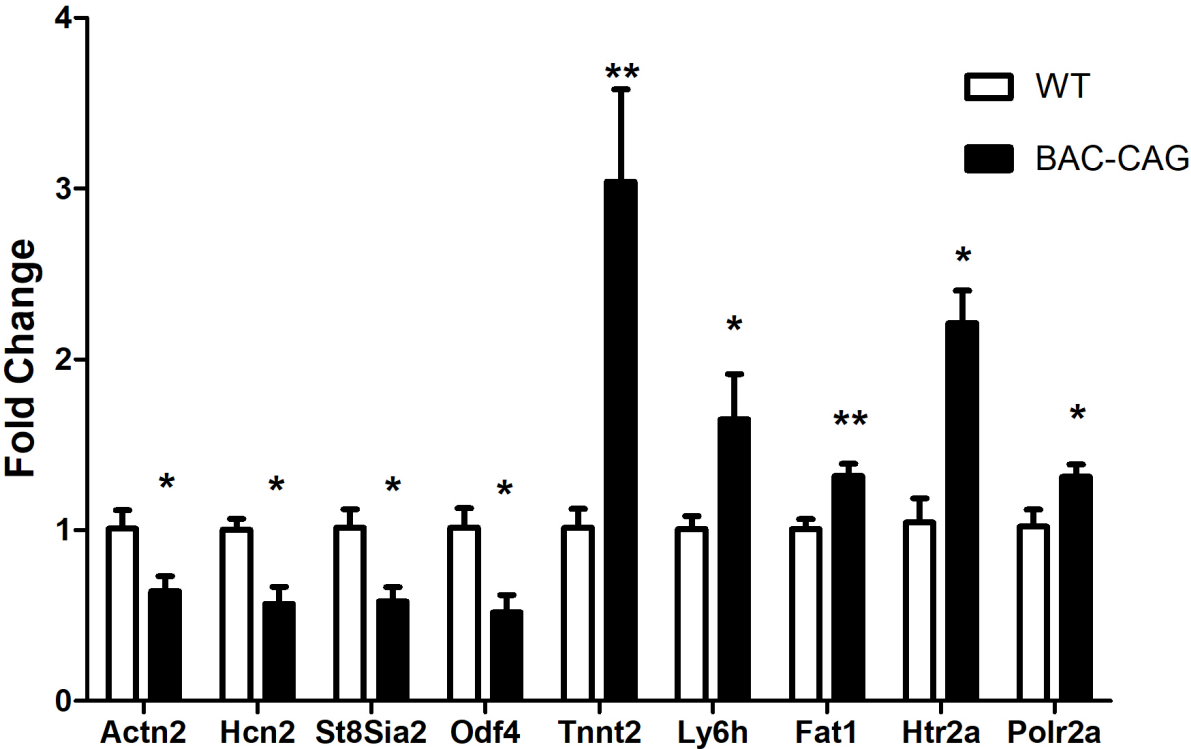
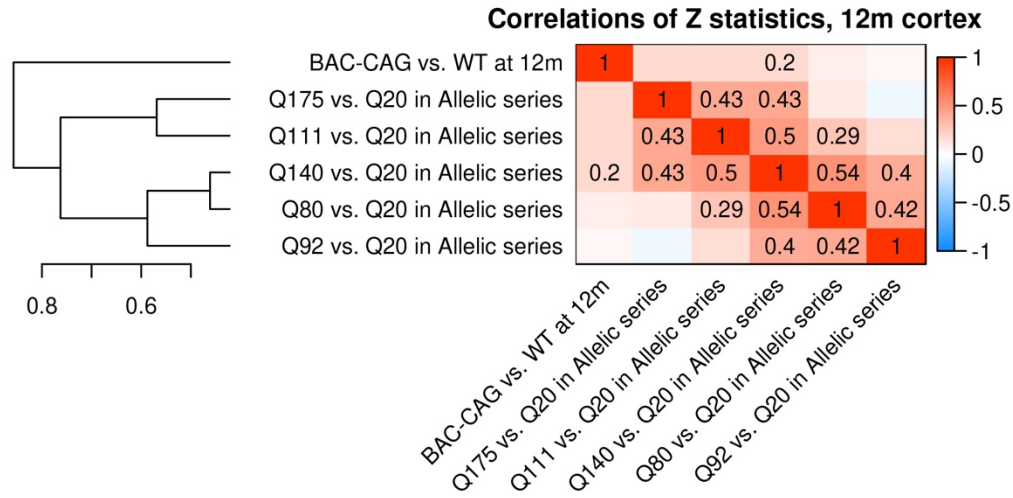


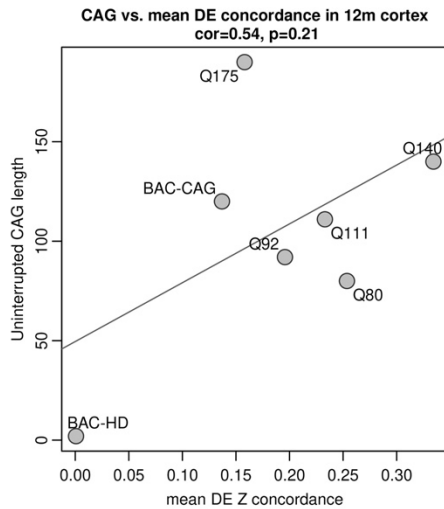
Figure S8 (Related to Figure 4). RT-qPCR confirmed some dysregulated gene expressions in 12m BAC-CAG brains.

Supplemental Figure S9

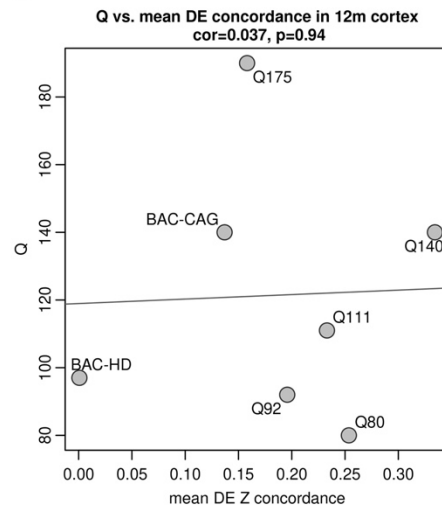
A



B



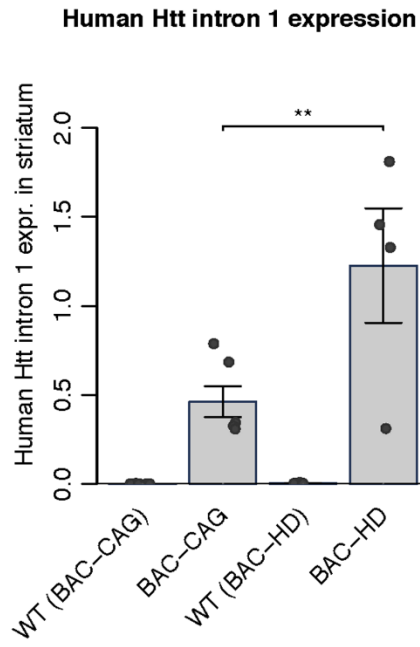
C



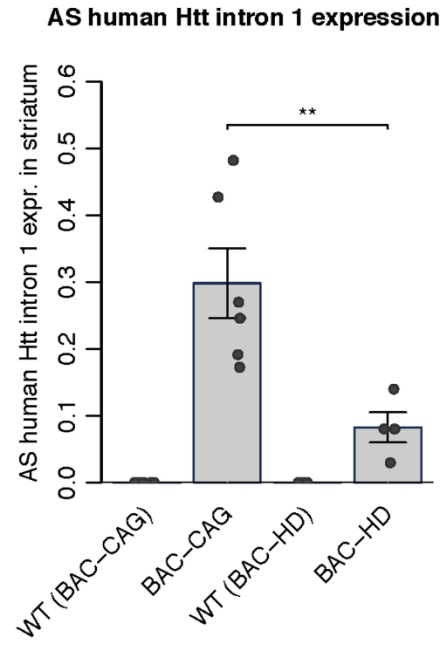
Supplemental Figure S9 (Related to Figure 5). Comparison of cortical transcriptionopathy between BAC-CAG and other full-length HD mouse models (A) Heatmap representation of genome-wide correlations of DE Z statistics of BAC-CAG mice (12m) and allelic series KI mice (6m). Correlations larger than 0.2 are also shown as numbers in the heatmap. The clustering tree on the left represents average-linkage hierarchical clustering based on the correlations. (B), (C) Scatterplots of uninterrupted CAG length (B) and Q-length (C) vs. mean concordance for each HD model (the mean concordance is the column-wise mean of the non-diagonal elements in the heatmap (A)). The plot in (B) includes the cortical DE gene concordance data from BAC-CAG, BACHD and the allelic series KI mice.

Supplemental Figure S10

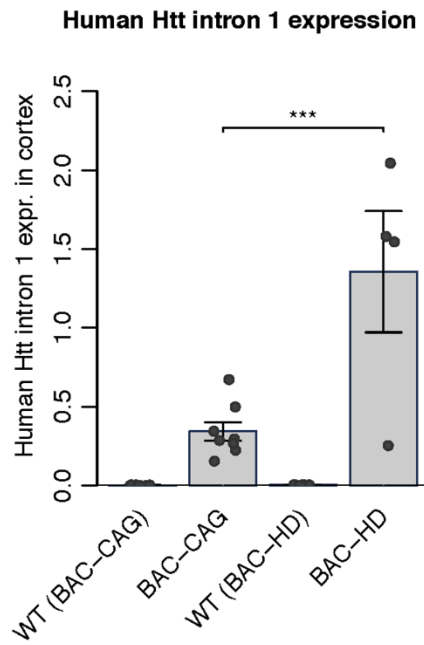
A



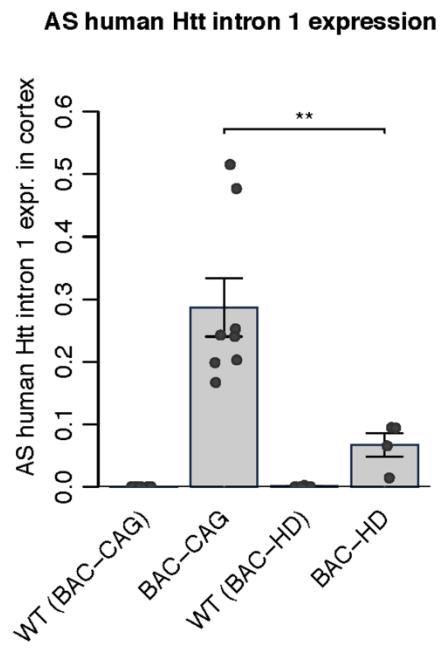
B



C



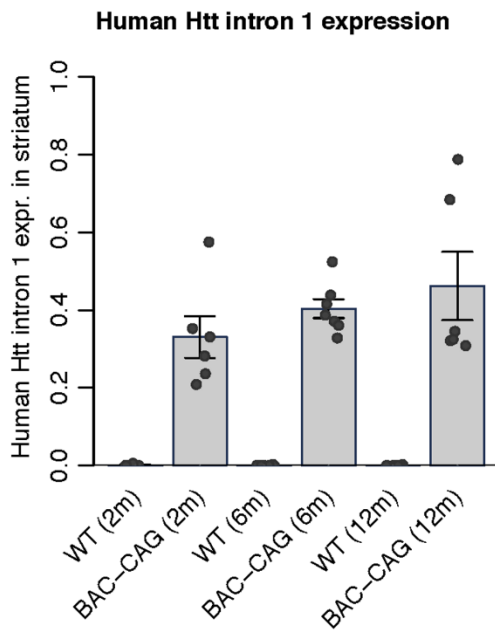
D



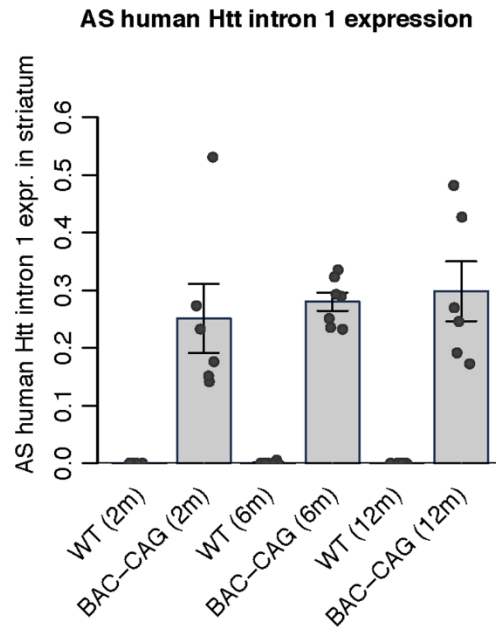
Supplemental Figure S10 (Related to Figure 7). Comparison of normalized total human *HTT* intron 1 and anti-sense (AS) intron 1 in striatum and cortex of 12-month BAC-CAG and BACHD from striatal and cortical transcriptomic study. Reads corresponding to *HTT* introns 1 and antisense intron1 (from 1 to 7397 nucleotides) from RNA-seq datasets were added for BAC-CAG and BACHD, respectively. (A) BACHD showed significantly higher human *HTT* intron1 reads compared to BAC-CAG, while BAC-CAG showed significant higher human *HTT* antisense transcript reads (B) in the striatum at 12m of age. Similarly in cortex BACHD had significant higher human *HTT* intron1 reads (C), while antisense intron1 reads was higher in BAC-CAG mice. Bars show means, error bars std. error of the mean and dots the individual observations ($n = 6$ per genotype except $n = 4$ for BACHD genotype). ANOVA followed by Tukey HSD test was used to test differences among the transgenic samples only. **: $p < 0.01$, ***: $p < 0.001$).

Supplemental Figure S11

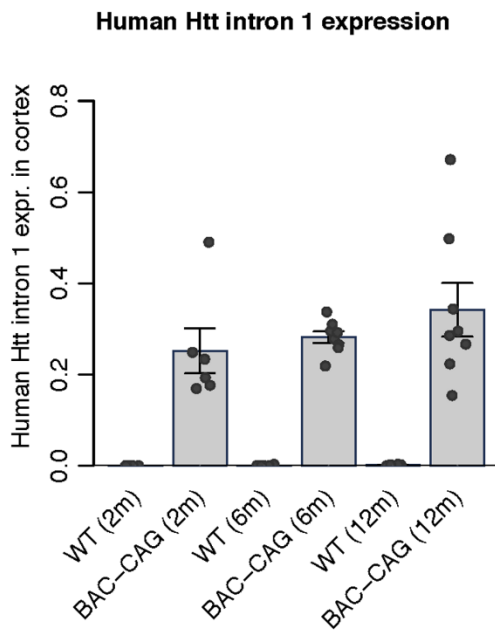
A



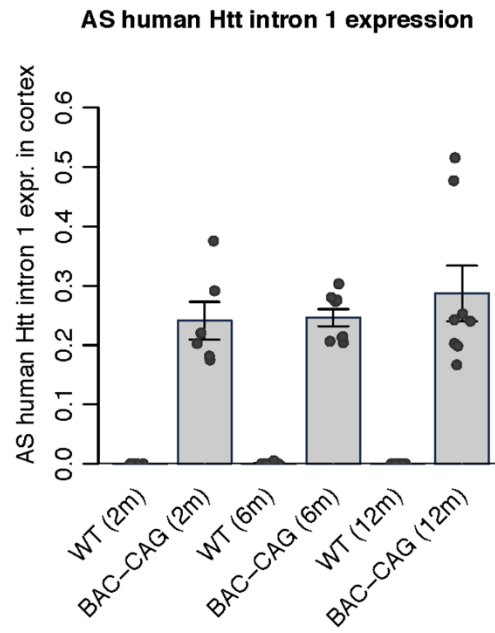
B



C



D



Supplemental Figure S11 (Related to Figure 7). *mHTT* Transcription levels were relatively stable in BAC-CAG brain tissues cross different age points. Reads corresponding to *HTT* introns 1 and antisense intron1 (from 1 to 7397 nucleotides) from 2m, 6m and 12m BAC-CAG RNA-seq datasets were added. Statistically no different among different age points for sense (A, C) and antisense (B, D) of *HTT* intron1 reads. ANOVA followed by Tukey HSD test was used to test differences among the transgenic samples only. Bars show means, error bars std. error of the mean and dots the individual observations ($n = 6$ per age points) **: $p < 0.01$, ***: $p < 0.001$).

Supplemental Figure S12

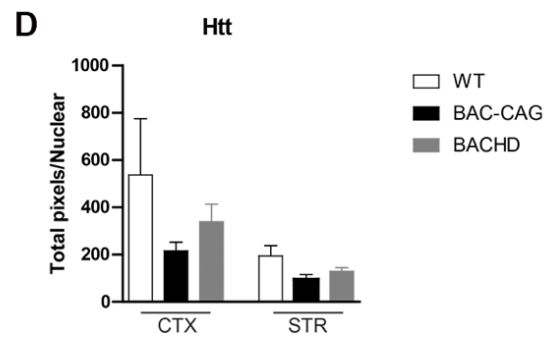
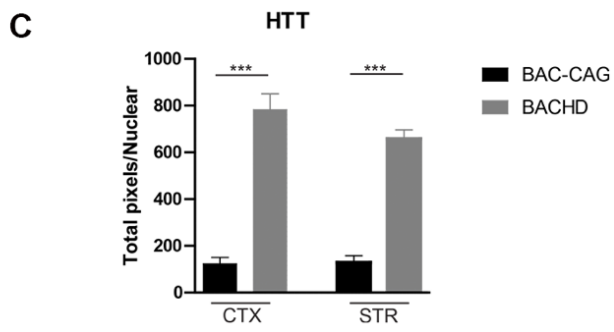
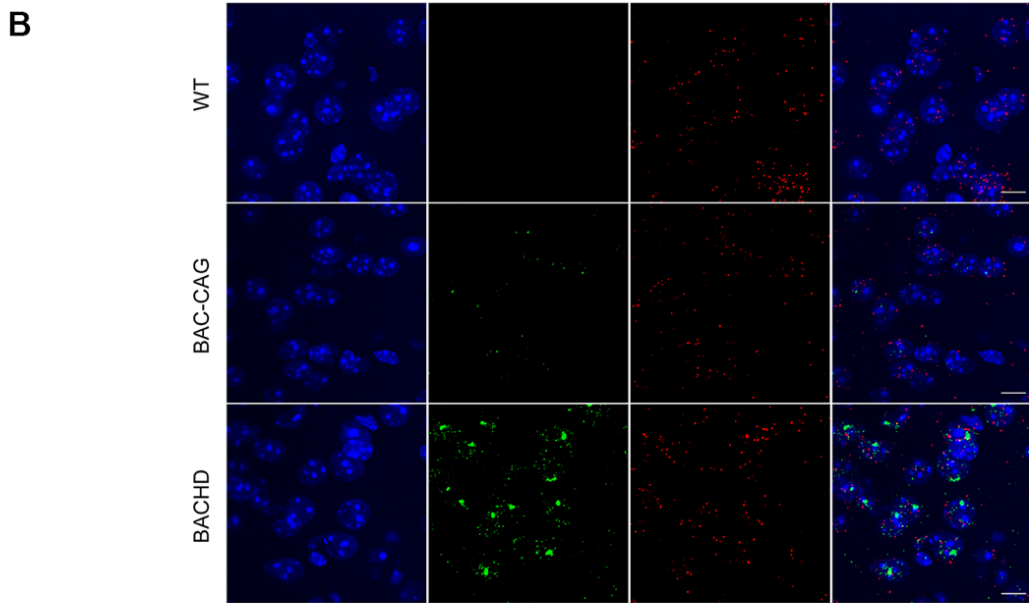
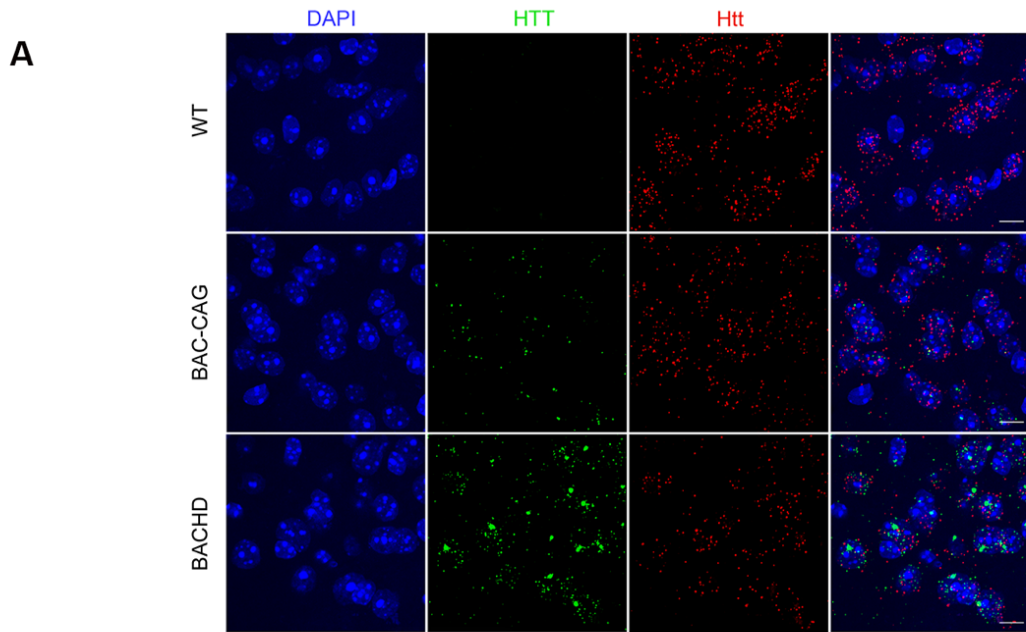


Figure S12 (Related to Figure 7). Significant higher of mHTT RNAs foci in cortex and striatum of BACHD mice. 20 μm thick brain sections from BAC-CAG and BACHD were probed with human HTT specific (cat#420231-C2, ACDBio) and mouse Htt specific (cat#473001, ACDBio) probes, respectively. Intensities of the foci in cortex (A) and striatum (B) were quantified using Imaris 9.2. (C) statistic significant nuclear retention of foci was detected in both cortex and striatum in BACHD mice compared to BAC-CAG mice (Unpaired t test. N=3 each for BAC-CAG, BACHD and WT), while no difference detected for mouse Htt (D). Results are shown as mean \pm SEM. Scale bars: 10 μm

Supplemental Figure S13

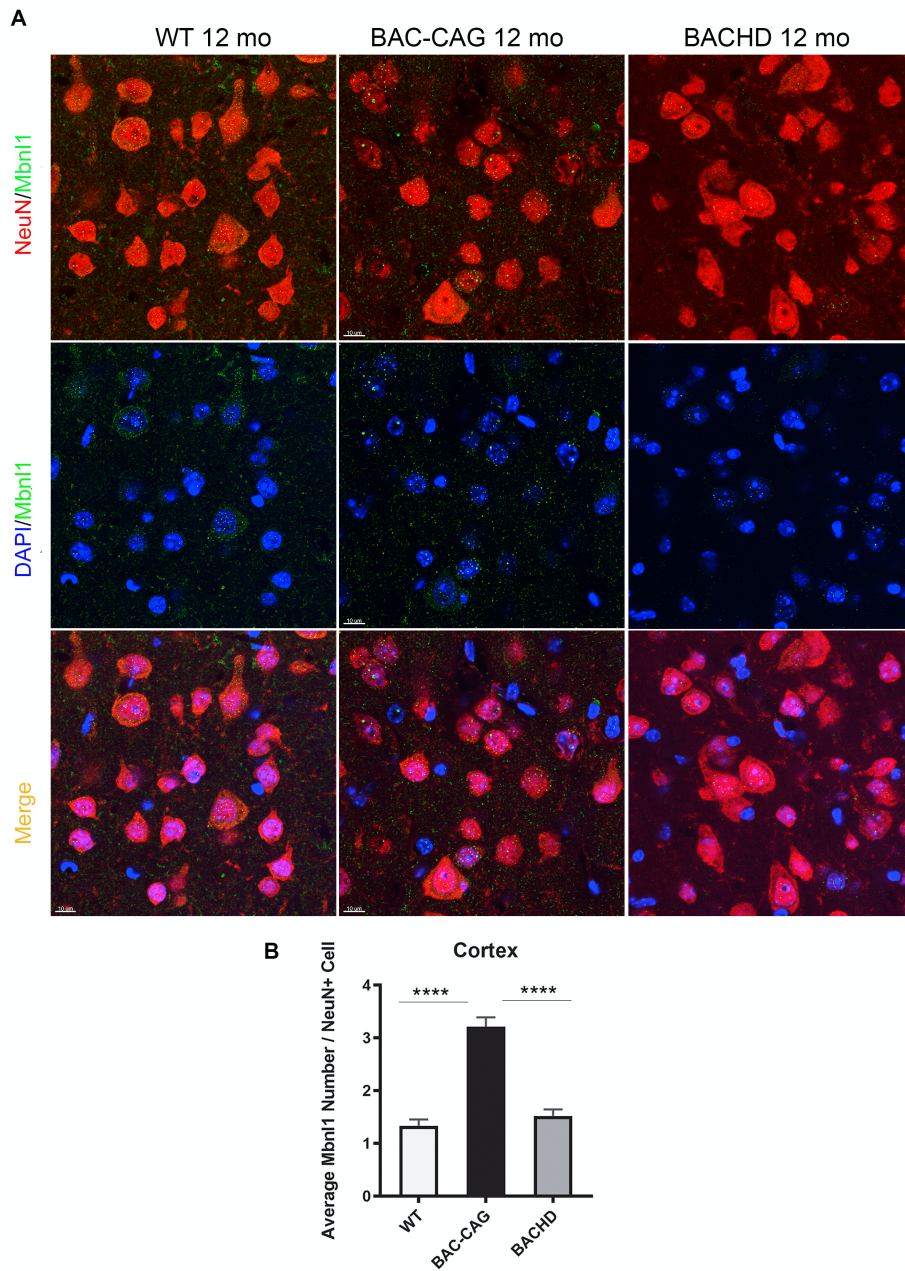


Figure S13 (Related to Figure 7). BAC-CAG mice exhibit brain wide cellular nuclear accumulations of Mbnl1. (A-B) BAC-CAG mice display significant more dot-like Mbnl1 nuclear accumulation in cortical cells compared with BACHD and WT mice, respectively. Results are shown as mean \pm SEM, $n=5$ for each age groups. ** $p<0.0001$; Scale bar: 10 μm .**

Supplemental Figure S14

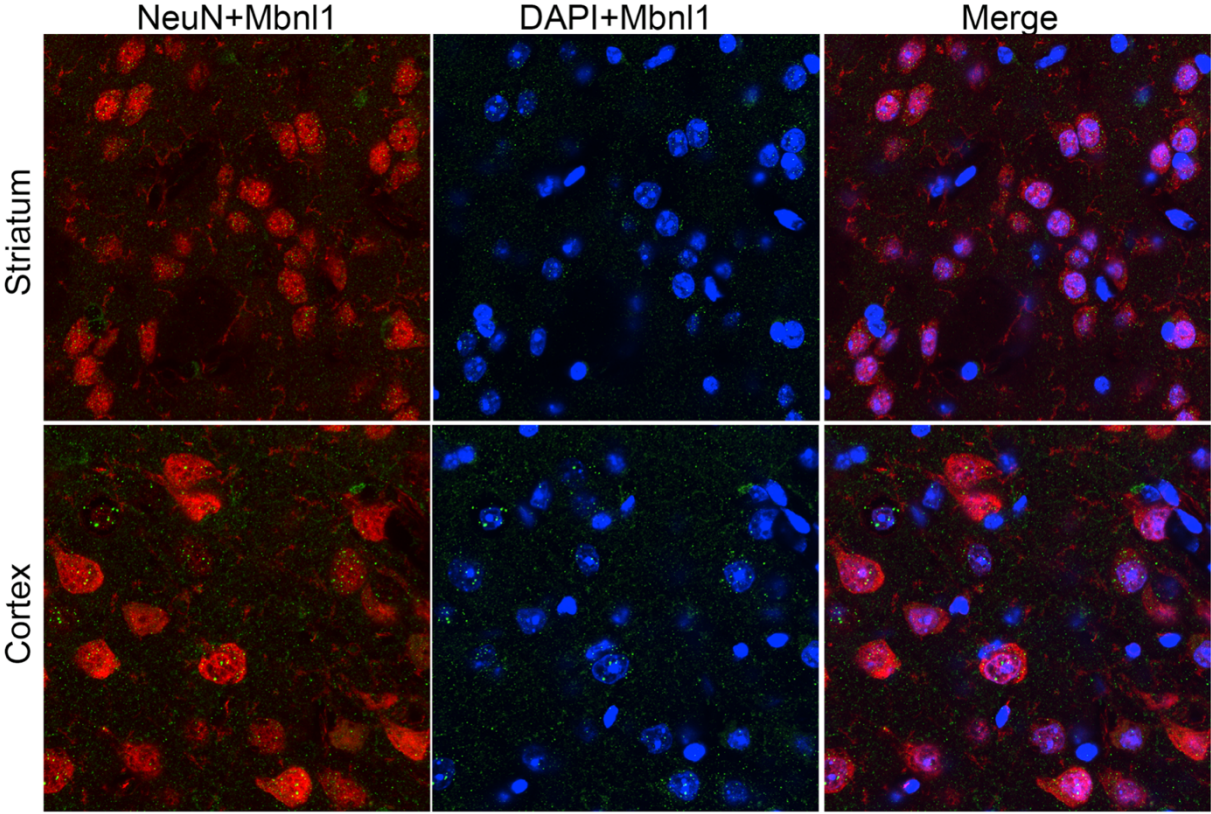


Figure S14 (Related to Figure 7). Q140 mice exhibit brain wide brain cells nuclear accumulation of Mbn11. Q140 mice at 12 month of old age display dot-like Mbn11 nuclear accumulation in striatal and cortical cells. Scale bar: 10 μ m

Supplemental Figure S15

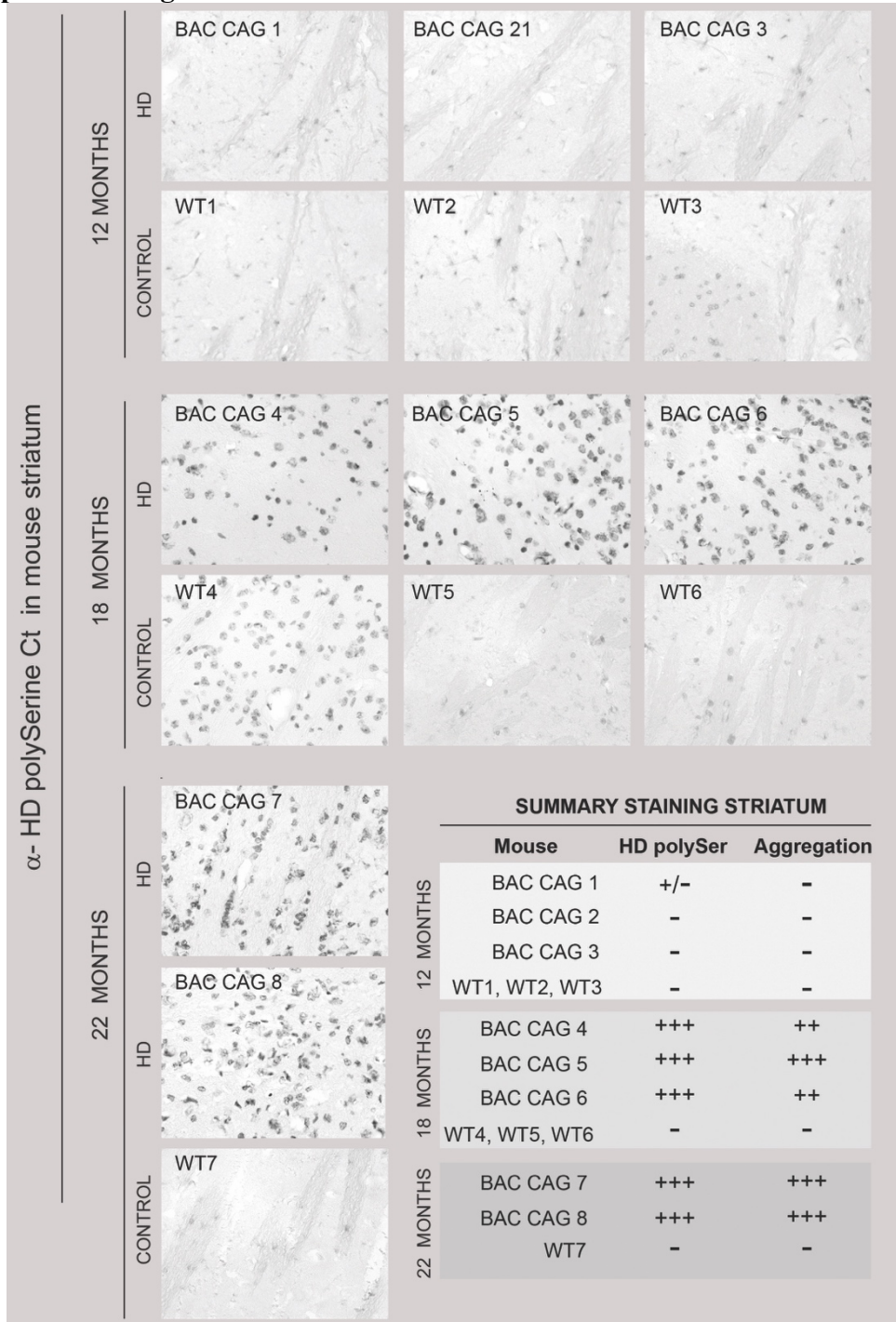


Figure S15 (Related to Figure 7). Late of age onset RAN translation in the striatum of BAC-CAG mice. No RAN proteins detected in BAC-CAG brains at 12m of age; at 18m of age polySer RAN products in aggregate and smear-like forms were detected in all brain regions of mouse brains including the striatum; we quantified RAN products in mouse striata and found the aggregate form of the RAN products increased as mice aged from 18m to 22m of ages.

Supplemental Figure S16

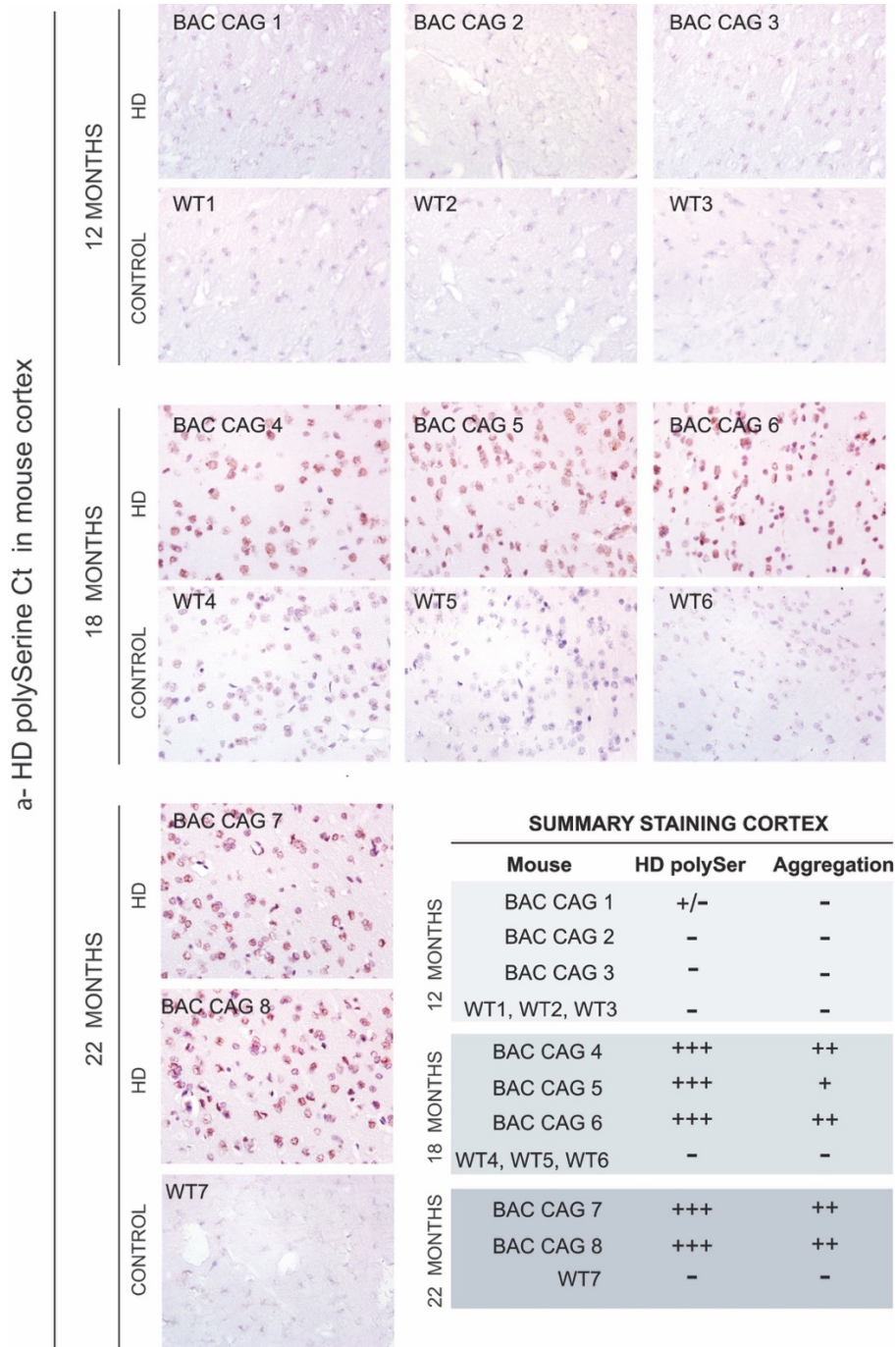


Figure S16 (Related to Figure 7). Late of age onset RAN translation in the cortex of BAC-CAG mice. No RAN proteins detected in BAC-CAG brains at 12m of age; at 18m of age polySer RAN products in aggregate and smear-like forms were detected in all brain regions of mouse brains including the cortices; we quantified RAN products in mouse cortices and found the aggregate form of the RAN products increased as mice aged from 18m to 22m of ages.

Supplemental Figure S17

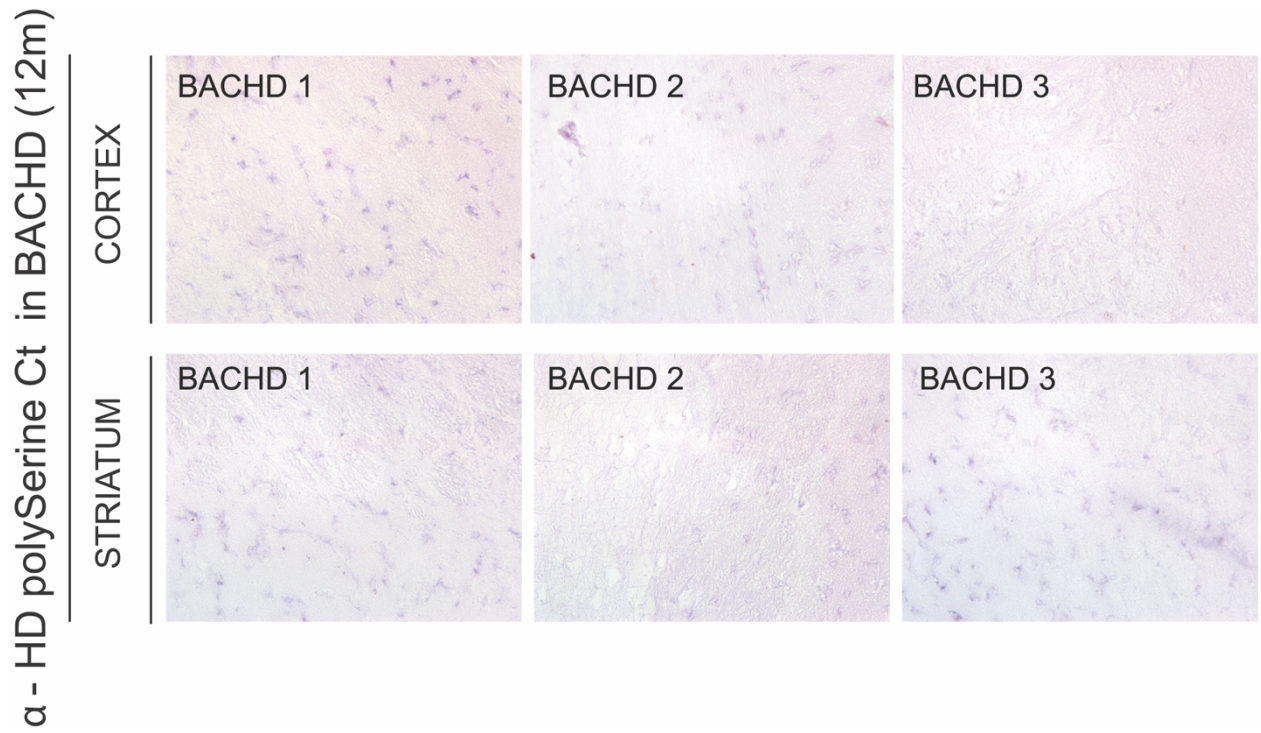


Figure S17 (Related to Figure 7). HD polySer RAN proteins were not detected in BACHD mouse cortex and striatum at 12m of age.

Supplemental Figure S18

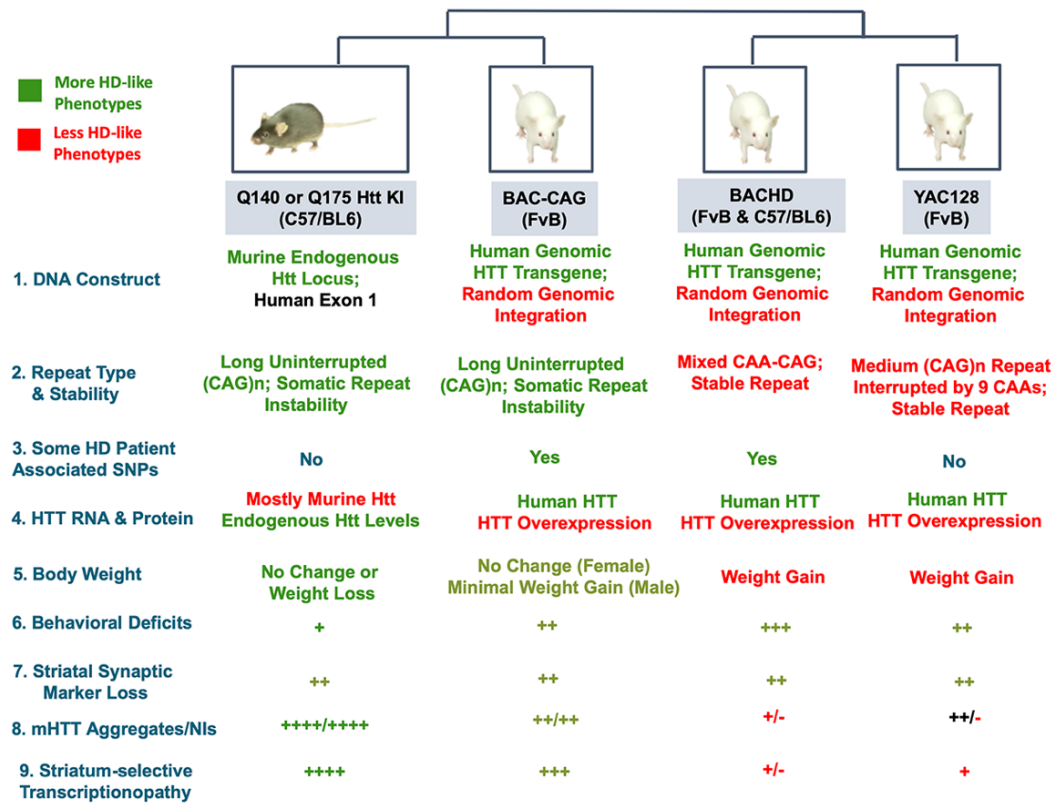


Figure S18 (Related to Figure 8). Clustering of human genomic transgenic mouse models and knockin mouse models of HD based on their similarity to (in green) or divergence from those found in HD patients. The models are clustered based on their overall similarity to each other.